Earth and Planetary Science Letters 501 (2018) 56–66

Contents lists available at ScienceDirect

Earth and Planetary Science Letters

www.elsevier.com/locate/epsl

Controls on subaerial erosion rates in Antarctica

Shasta M. Marrero [a,*], Andrew S. Hein [a], Mark Naylor [a], Mikael Attal [a], Richard Shanks [b], Kate Winter [c], John Woodward [c], Stuart Dunning [d], Matthew Westoby [c], David Sugden [a]

[a] School of GeoSciences, University of Edinburgh, Drummond Street, EH8 8XP, UK
[b] Scottish Universities Environmental Research Centre, East Kilbride, UK
[c] Department of Geography and Environmental Sciences, Faculty of Engineering and Environment, Northumbria University, Newcastle upon Tyne, UK
[d] Department of Geography, School of Geography, Politics, and Sociology, Newcastle University, Newcastle upon Tyne, UK

ARTICLE INFO

Article history:
Received 28 April 2018
Received in revised form 3 August 2018
Accepted 8 August 2018
Available online xxxx
Editor: A. Yin

Keywords:
erosion rate
cosmogenic nuclides
chlorine-36
lithology
Antarctica

ABSTRACT

Erosion rates offer insight on landscape development and the relative importance of chemical and physical processes of weathering. Minimal chemical weathering makes Antarctica an ideal location in which to compare the physical weathering of carbonate rocks to other lithologies. Here we report the first cosmogenic nuclide-derived erosion rates for carbonate rocks in Antarctica. Carbonate samples collected in the southernmost Ellsworth Mountains reflect a ^{36}Cl erosion rate of 0.22 ± 0.02 mm/ka. This erosion rate is consistent with other reported Antarctic erosion rates, but is lower than ^{36}Cl erosion rates derived from other arid regions in the world. These results are integrated with a continent-wide reanalysis of 28 cosmogenic nuclide erosion rate studies (>200 measurements), which comprise numerous rock types and multiple cosmogenic nuclides. By combining cosmogenic nuclide-derived erosion rates across studies, the larger trends provide insight into factors (e.g. lithology, glacial history, and availability of abrasive material) affecting subaerial erosion rates in Antarctica. Statistical analysis of the compiled data set shows differences based on lithology, with sandstone having the largest range of erosion rates. The compiled data also reveals higher erosion rates in areas with a large potential sediment supply, like the Dry Valleys. Samples collected from boulders yield lower erosion rates than those collected from bedrock, likely due to a combination of physical processes that affect boulders and bedrock differently, and glacial history, which can affect the apparent cosmogenic-nuclide derived erosion rate.

© 2018 The Authors. Published by Elsevier B.V. This is an open access article under the CC BY license (http://creativecommons.org/licenses/by/4.0/).

1. Introduction

Quantification of erosion rates has been crucial in developing our understanding of how landscapes evolve. Erosion rate data allow the reconstruction of the time evolution of landscapes on a range of scales. Data has been used to test models of landscape evolution and river erosion at the basin scale (e.g., Tomkin et al., 2003; van der Beek and Bishop, 2003) and on a global scale – to establish the relationships and feedbacks between climate, tectonics, lithology and erosion (Harel et al., 2016; Molnar and England, 1990; Peizhen et al., 2001; Portenga and Bierman, 2011). Effects on reported erosion rates include precipitation (Bierman and Caffee, 2002), temperature, climate (Bookhagen and Strecker, 2012), altitude, vegetative state, presence/absence of soil (Heimsath et al., 1999; Stephenson and Finlayson, 2009), and the time period of measurement (Hewawasam et al., 2003). Although lithology clearly influences erosion rates, quantitative assessment of changes across different rock types have been hindered by these variables (Ryb et al., 2014), with carbonate rocks posing a particular challenge due to the contribution of chemical dissolution.

Cosmogenic nuclides, which accumulate in rocks exposed at the Earth's surface, enable the determination of exposure ages over a range of time and space scales, from thousands to millions of years, and erosion rates from outcrop to basin-wide scale (e.g., Bierman and Steig, 1996; Granger et al., 1996; Niedermann, 2002). The calculation of cosmogenic nuclide-derived exposure ages is highly sensitive to the rock surface erosion rate because the exposure age behaves non-linearly with erosion rate (Lal, 1991); thus even low erosion rates can dramatically increase the calculated ages of old surfaces, such as those present in Antarctica (e.g., Fink et al., 2006; Margerison et al., 2005). Improved erosion rate determinations are therefore a critical step to improve the reliability of exposure ages.

Minimal chemical weathering makes Antarctica an ideal location in which to compare the physical weathering of carbonate

* Corresponding author.
E-mail address: shasta.marrero@ed.ac.uk (S.M. Marrero).

https://doi.org/10.1016/j.epsl.2018.08.018
0012-821X/© 2018 The Authors. Published by Elsevier B.V. This is an open access article under the CC BY license (http://creativecommons.org/licenses/by/4.0/).

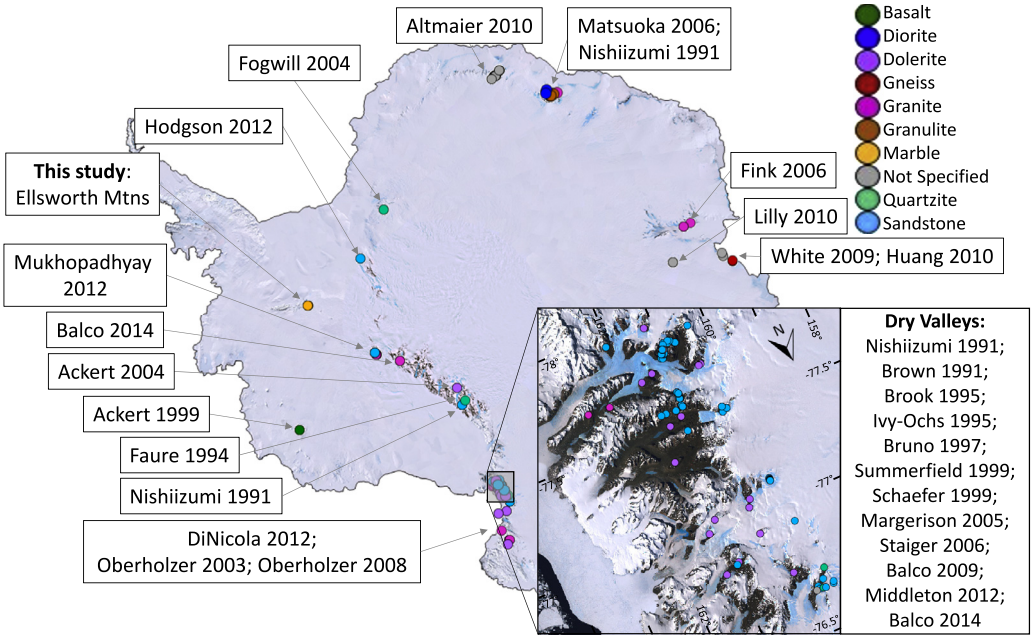

Fig. 1. Locations of all Antarctic erosion rate studies compiled for this paper. Full references are: Ackert (1999), Ackert and Kurz (2004), Altmaier et al. (2010), Balco and Shuster (2009), Balco et al. (2014), Bromley et al. (2010), Brook et al. (1995), Brown et al. (1991), Bruno et al. (1997), Di Nicola et al. (2012), Fink et al. (2006), Fogwill et al. (2004), Hodgson et al. (2012), Huang et al. (2010), Ivy-Ochs et al. (1995), Kiernan et al. (2009), Lilly et al. (2010), Margerison et al. (2005), Matsuoka et al. (2006), Middleton et al. (2012), Mukhopadhyay et al. (2012), Nishiizumi et al. (1991), Oberholzer et al. (2008), Oberholzer et al. (2003), Schaefer et al. (1999), Staiger et al. (2006), Summerfield et al. (1999), Swanger et al. (2011), White et al. (2009). Background image: Landsat Image Mosaic of Antarctica. Lithology is indicated by different colours. (For interpretation of the colours in the figure(s), the reader is referred to the web version of this article.)

rocks to other lithologies. Published Antarctic erosion rate data have been derived from a range of rock types exposed in ice-free areas across the continent. These data provide an opportunity to investigate the systematic controls on physical erosion rates and processes in a unique environment that is comparatively free from complicating variables that typically affect similar studies in temperate regions of the world. As a result erosion rates measured in Antarctica are amongst the lowest documented on Earth (Nishiizumi et al., 1991; Portenga and Bierman, 2011). The polar climate limits chemical weathering and freeze-thaw processes since samples are exposed to liquid water less frequently than in temperate climates. Soil and vegetation, which can complicate measurements and increase erosion rates, are virtually nonexistent in many locations in Antarctica (Weyant, 1966). Finally, due to a comparatively reduced presence of liquid water in Antarctica, solutional erosion of carbonate rocks are minimised, making Antarctica an ideal location to examine the physical erosion of carbonate bedrock.

Here we compile and reanalyse 28 studies reporting 283 independent analyses, representing Antarctic cosmogenic studies published prior to 2015. We review cosmogenic nuclide-derived subaerial erosion rates from the continent and investigate the variables influencing erosion rates and the physical processes at work. Of the sampled Antarctic nunataks and other ice-free areas (Fig. 1), >55% of the samples derive from the Dry Valleys. These analyses are made up of ^{10}Be (32%), ^{26}Al (24%), ^{21}Ne (26%), ^{3}He (15%), and ^{36}Cl (3%, basalts only), where many studies have incorporated more than one nuclide to measure erosion rates on bedrock outcrops and/or boulders. These studies have focused on either quartz-bearing lithologies (e.g. sandstone, granite) using cosmogenic ^{10}Be, ^{26}Al and ^{21}Ne, or dolerite using ^{21}Ne and ^{3}He in olivines. Carbonate rocks have never been analysed. In this paper, we present the first cosmogenic ^{36}Cl erosion rates on Antarctic carbonate rocks.

2. Methods

2.1. Carbonate erosion rate methods and field site

Erosion rates were derived from carbonate bedrock in the southern Heritage Range, Ellsworth Mountains, in the Weddell Sea sector of the West Antarctic Ice Sheet (Fig. 2). The Marble Hills field site is located ~50 km from Hercules Inlet, where continental ice drains into the floating Filchner-Ronne Ice Shelf (Fig. 2b). The massif includes high peaks with steep slopes that contrast with the lower flank of the massif, which is characterised by low-angled, ice-moulded bedrock, draped with glacial erratics and till.

Carbonate samples were collected from ice-moulded, smooth bedrock surfaces at three sites in the Marble Hills. At the first site, four samples (MH12-30, 31, 32, and the top sample from a 1.5 m vertical bedrock core) were collected from the top of a high (1380 m), ice-moulded bedrock dome (informally named Marble Dome) situated on the northern side of the Marble Hills massif (Fig. 2a/2c). The site sits above the upper-limit of ice cover during the Last Glacial Maximum (Bentley et al., 2010; Hein et al., 2016a), where cosmogenic ^{26}Al/^{10}Be and ^{21}Ne/^{10}Be ratios in glacial erratics indicate that the dome summit has been largely exposed for 600–700 ka (Hein et al., 2016b). At the second site, three samples (MH12-68, 69, 70) were collected from a narrow ridge on the summit of the highest peak in Marble Hills massif, Mt. Fordell, which stands 1680 m above sea level (Fig. 2a/2d). Cosmogenic ^{26}Al/^{10}Be and ^{21}Ne/^{10}Be ratios in glacial erratics on a depositional trimline (situated ~300 m below the summit, Sugden et al., 2017) indicate that the upper slopes of Marble Hills have been exposed for at least ~1.4 Ma (Hein et al., 2016b). The final 'site' represents a group of seven samples (MH12-75 and all six MH14 samples) collected from glacial drift-covered bedrock exposed at lower elevations, ranging from c. 1340–1160 m down to the modern ice elevation. In this area, geomorphological evidence implies repeated episodes of ice cover (Hein et al., 2016b), although the specific chronology of each location is unknown. We

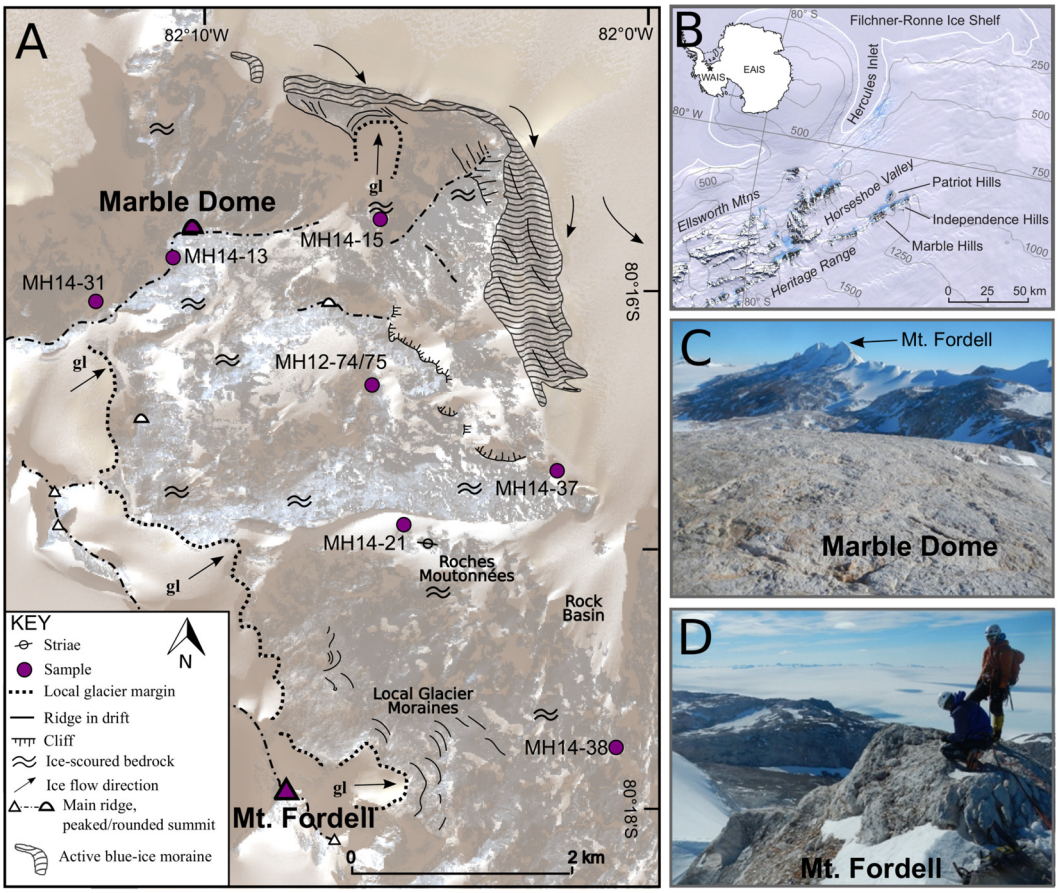

Fig. 2. (A) Location map for carbonate bedrock samples in the Marble Hills, Ellsworth Mountains, Antarctica. Sample locations are shown individually for all samples not located at either Marble Dome or Mt. Fordell. (B) Map of region surrounding Marble Hills. (C) View from Marble Dome (smooth, ice-moulded surface in the foreground) towards Mt. Fordell (highest peak in the background). (D) Photo of sample collection on Mt. Fordell.

note that cover by ice serves only to increase the apparent maximum erosion rate, thus, while this site can still provide valuable maximum limiting erosion rates in an area with no other constraints, it does not accurately represent the best estimate of subaerial erosion rates in the region.

Approximately 1–2 kg of calcite vein or marbleised limestone bedrock was removed from the top 2–5 cm of the bedrock surface by hammer and chisel. Topographic shielding was measured with a clinometer and locational information was obtained with a hand-held GPS unit. Field photos of samples and sample sites are shown in Fig. 2 and Supplementary Figs. S1–S12.

The cosmogenic ^{36}Cl samples were processed at the University of Edinburgh using procedures fully described in the Supplementary Information. Sample location and composition information are provided in Table 1, with additional information including the accelerator mass spectrometry (AMS) results available in the Supplementary Spreadsheet. All samples contain low native Cl concentrations (Table 1), so production is dominated by Ca spallation (>93%). Blank subtractions for native Cl were sometimes a large portion (40%) of the total Cl concentration due to low concentrations in the original rock. Blank subtractions for ^{36}Cl were generally small (<5%) and applied to the samples based on process blanks from each sample batch (see Supplementary Spreadsheet). The first batch of samples did not include sufficient carrier, which caused them to be out of the calibrated measurement range for the AMS. These samples are excluded from all analyses although they are included in the Supplementary Spreadsheet.

Erosion rates were calculated using CRONUScalc (Marrero et al., 2016a), which uses CRONUS-Earth production rates (Borchers et al., 2016; Marrero et al., 2016b; Phillips et al., 2016) to numerically model the nuclide concentration with different erosion rates until CRONUScalc matches the measured sample concentration.

We calculate erosion rates for both 'infinite exposure' and 'minimum exposure' scenarios. The infinite exposure method assumes that each sample has been exposed for many half-lives beyond what is necessary to reach erosional equilibrium, which yields the maximum limiting erosion rate for the sample. The second method uses information on the minimum exposure duration of the sample site; this scenario generally yields a lower bound on the erosion rate because the measured nuclide concentration is achieved in a shorter exposure time. The true erosion rate likely falls between the 'infinite' and 'minimum exposure' scenario estimates due to the potential effects of burial by cold-based ice and inheritance (applies to minimum-exposure only). Minimum exposure ages for Mt. Fordell (1350 ka; sample MH12-68) and Marble Dome (660 ka; samples MH12-30, 31, 32, C1-TO) were derived from cosmogenic nuclide-dated (^{10}Be and ^{26}Al) erratics (Lal (1991)/Stone (2000) scaling assuming zero erosion) (Hein et al., 2016a, 2016b). Given the long half-lives of ^{10}Be and ^{26}Al, we cannot rule out periods of burial during the exposure history, but this is unimportant given that these parameters are only used as limiting bounds on the erosion rate. The minimum-exposure scenario yields some results where samples are oversaturated with respect to zero erosion, indicating that zero is the minimum erosion bound for these samples. For this reason and consistency with other publications, the maximum erosion rate (assuming infinite exposure) is used for the interpretation of all results.

Table 1
Location, composition, and other relevant parameters for the calculation of ^{36}Cl erosion rates.

Name	Units	Uncerts	MH12-68	MH12-30A	MH12-30B	MH12-31	MH12-32	MH12-C1-TO
Sample type			marbleised LS	calcite vein	calcite vein	marbleised LS	calcite vein	marbleised LS
Latitude	dd	0	−80.30576	−80.26309	−80.26309	−80.26309	−80.26309	−80.26334
Longitude	dd	0	−82.11405	−82.18705	−82.18705	−82.18705	−82.18705	−82.18677
Elevation	m	5	1681	1381	1381	1381	1381	1393
Pressure	hPa	10	793	826	826	826	826	825
Thickness	cm	0.5	1.5	1	1	4.5	1	5
Bulk density	g/cm^3	0.1	2.55	2.71	2.71	2.55	2.71	2.55
Shielding	unitless	0	1.000	1.000	1.000	1.000	1.000	1.000
Conc. ^{36}Cl	at ^{36}Cl/g (x1E6)		42.3 ± 1.2	39.8 ± 1.2	37.1 ± 1.0	33.88 ± 0.97	38.3 ± 1.1	34.6 ± 1.5
SiO_2	bulk wt%	1.67	0.28 ± 0.2	0.51	0.51	0.55 ± 0.2	0.39 ± 0.2	0.41
TiO_2	bulk wt%	0.04	0 ± 0.02	0	0	0.01 ± 0.02	0 ± 0.02	0.01
Al_2O_3	bulk wt%	0.03	0.02 ± 0.03	0.02	0.02	0.11 ± 0.03	0.04 ± 0.03	0.06
Fe_2O_3	bulk wt%	0.17	0.06 ± 0.03	0.19	0.19	0.29 ± 0.03	0.11 ± 0.03	0.17
MnO	bulk wt%	0.02	0.02 ± 0.01	0.05	0.05	0.02 ± 0.01	0.06 ± 0.01	0.02
MgO	bulk wt%	3.93	0.44 ± 0.4	0.24	0.24	0.25 ± 0.4	0.1 ± 0.4	0.34
CaO	bulk wt%	6.3	56.6 ± 0.8	55.56	55.56	55.69 ± 0.8	54.53 ± 0.8	56.15
Na_2O	bulk wt%	0.04	0.07 ± 0.03	0.01	0.01	0.02 ± 0.03	0 ± 0.03	0.04
K_2O	bulk wt%	0.18	0.01 ± 0.01	0.01	0.01	0.02 ± 0.01	0 ± 0.01	0.02
P_2O_5	bulk wt%	0.04	0.03 ± 0.04	0.01	0.01	0.09 ± 0.04	0 ± 0.04	0.06
CO_2	bulk wt%	0.61	43.4 ± 0.4	44.11	44.11	43.39 ± 0.4	44.71 ± 0.4	43.4
Sm	bulk ppm	0.5	0.1 ± 0.1	0.42	0.42	0.42	0.42	0.42
Gd	bulk ppm	0.57	0.13 ± 0.05	0.41	0.41	0.41	0.41	0.41
U	bulk ppm	2.53	2.72 ± 0.05	1.16	1.16	1.16	1.16	1.16
Th	bulk ppm	2.1	0 ± 0.1	0.58	0.58	0.58	0.58	0.58
Cr	bulk ppm	23	0 ± 5	7.4	7.4	7.4	7.4	7.4
Li	bulk ppm	7	0 ± 5	1.4	1.4	1.4	1.4	1.4
Target K_2O	tar wt%	0.01	5.0E−04	4.4E−04	1.1E−03	1.1E−03	7.8E−04	3.1E−03
Target CaO	tar wt%	2	53.7	55.0	57.4	52.3	52.2	54
Target TiO_2	tar wt%	0.02	1.7E−05	0.0E+00	7.7E−07	2.0E−05	3.3E−05	2.0E−05
Target Fe_2O_3	tar wt%	0.2	8.8E−03	2.3E−03	3.3E−03	2.0E−02	4.3E−02	1.6E−02
Target Cl	tar ppm		5.0 ± 4.3	20.9 ± 1.4	17.6 ± 1.1	15.6 ± 1.4	36.5 ± 1.4	14.7 ± 9.3
Covariance	unitless		909	2133	1525	1422	4571	1118

Name	MH14-13	MH14-31	MH12-75	MH14-15	MH14-38	MH14-21	MH14-37
Sample type	marbleised LS	marbleised LS	marbleised LS	marbleised LS	marbleised LS	str marbleised LS	str marbleised LS
Latitude	−80.2642	−80.26735	−80.27371	−80.26105	−80.29905	−80.28305	−80.2794
Longitude	−82.18933	−82.21628	−82.10712	−82.10672	−82.00345	−82.097926	−82.02958
Elevation	1343	1273	1163	1102	826	746	809
Pressure	830	838	851	858	890	901	893
Thickness	2.5	1.75	2	2	3.5	1	3
Bulk density	2.55	2.55	2.55	2.55	2.55	2.55	2.55
Shielding	0.994	0.994	1.000	0.998	0.991	0.979	0.975
Conc. ^{36}Cl	31.6 ± 1.3	29.2 ± 1.2	24.58 ± 0.69	13.05 ± 0.54	3.72 ± 0.15	2.94 ± 0.13	0.438 ± 0.023
SiO_2	1.1	1.1	0.41	1.1	1.1 ± 0.2	2.35	1.89
TiO_2	0.01	0.01	0.01	0.01	0.01 ± 0.02	0.04	0.04
Al_2O_3	0.28	0.28	0.06	0.28	0.28	0.79	0.55
Fe_2O_3	0.1	0.1	0.17	0.1	0.1 ± 0.03	0.31	0.28
MnO	0.02	0.02	0.02	0.02	0.02 ± 0.01	0.01	0.01
MgO	0.7	0.7	0.34	0.7	0.7 ± 0.4	4.34	3.14
CaO	54.4	54.4	56.15	54.4	54.4 ± 0.03	49.26	51.24
Na_2O	0	0	0.04	0	0 ± 0.01	0.04	0.05
K_2O	0.05	0.05	0.02	0.05	0.05 ± 0.01	0.21	0.17
P_2O_5	0.03	0.03	0.06	0.03	0.03 ± 0.04	0.03	0.03
CO_2	43.25	43.25	43.4	43.25	43.25 ± 0.4	42.98	43.04
Sm	0.42	0.42	0.42	0.42	0.42	0.42	0.42
Gd	0.41	0.41	0.41	0.41	0.41	0.41	0.41
U	1.16	1.16	1.16	1.16	1.16	1.16	1.16
Th	0.58	0.58	0.58	0.58	0.58	0.58	0.58
Cr	7.4	7.4	7.4	7.4	7.4	7.4	7.4
Li	1.4	1.4	1.4	1.4	1.4	1.4	1.4
Target K_2O	4.3E−03	2.6E−03	1.6E−03	5.1E−03	2.8E−03	2.7E−03	7.6E−03
Target CaO	59.3	53.9	52.7	53.6	53.5	56.0	53.5
Target TiO_2	3.0E−05	1.1E−05	9.6E−06	2.5E−05	1.8E−05	7.9E−05	8.6E−05
Target Fe_2O_3	2.8E−02	2.1E−02	1.8E−02	6.6E−02	3.3E−02	4.2E−02	3.5E−02
Target Cl	8.7 ± 2.8	9.4 ± 2.8	20.0 ± 1.4	7.5 ± 2.4	5.9 ± 2.2	7.0 ± 2.0	20.9 ± 2.3
Covariance	596	566	3568	212	51	48	22

Raw data for the Accelerator Mass Spectrometry values, blank subtraction, and carrier information are included in the Supplementary Spreadsheet. Samples are all surface samples and were collected in 2012 or 2014 according to sample name. Pore water, analytical water, and boron concentrations are all zero. Pressure and attenuation length (153 g/cm^2) are calculated according to CRONUScalc (Marrero et al., 2016a). Sample type includes specific descriptions of the sample including whether it was a calcite vein, marbleised limestone (LS), or striated (str). Bulk density is estimated from lithology: calcite as 2.71 g/cm^3 and marbleised limestone as 2.55 g/cm^3. Bulk rock major elements were measured via XRF at the University of Edinburgh, School of GeoSciences. Bulk rock trace elements were measured via ICP-OES at SGS Mineral Services, Inc. (Canada). Target concentrations were measured via ICP-OES at the University of Edinburgh, School of Chemistry. AMS measurements were performed at SUERC. This provides the data to calculate ^{36}Cl and Cl concentrations according to the procedure described in the Supplemental Information. Bulk and target Cl concentrations are assumed to be equal. Uncertainty is given for all unique values; otherwise, uncertainties are provided in the 'Uncerts' column of the table.

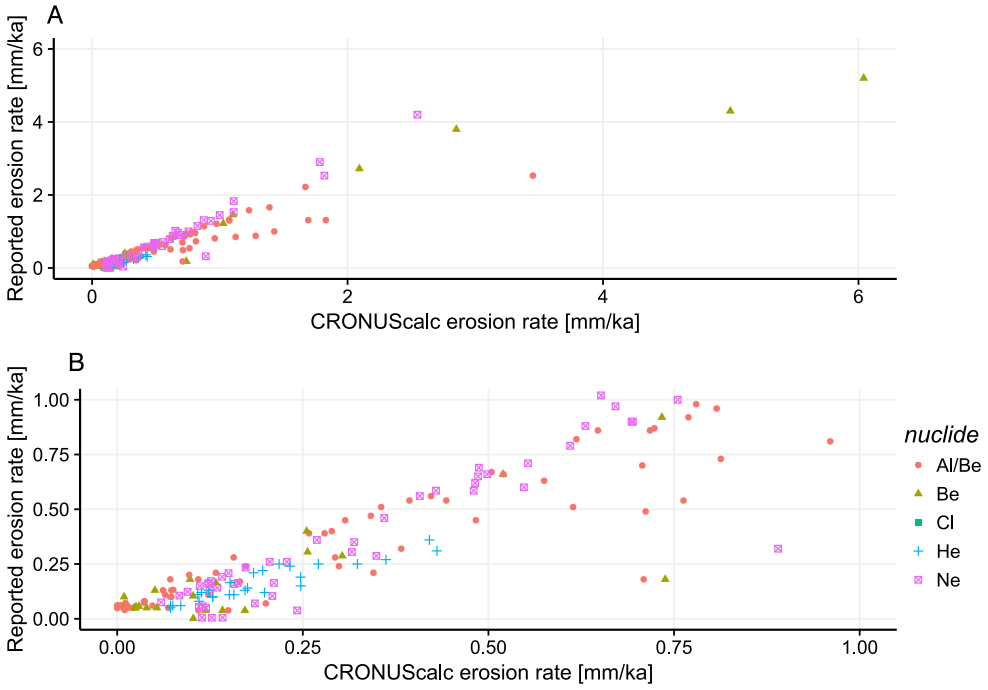

Fig. 3. Comparison of originally reported values to the recalculated erosion rates from CRONUScalc. Nuclides are indicated by different symbols. Dashed line indicates the 1:1 line. (A) Full set of erosion rates and (B) detail in the range up to 1 mm/ka.

2.2. Erosion rate compilation methods

Specific selection criteria were adopted to produce the compilation of Antarctic-wide erosion rate data. Only samples determined by the original studies as representative of erosion rates were included (i.e., outliers excluded in the original studies were also excluded here). Sample information used in the compilation was taken from the ICE-D database (http://antarctica.ice-d.org/) or from the original publication. Authors were contacted to provide any missing information and excluded if this was not successful. Any samples identified as 'complex exposure' samples by the authors, as determined from disagreement between ^{10}Be and ^{26}Al results, were also removed. ^{26}Al results are not reported here because authors tended to exclude all samples with differences between results from ^{10}Be and ^{26}Al as complex exposure samples, so they present no unique data. The complete list of publications, calculator inputs, included/excluded samples, reproducibility study, and a detailed discussion of multi-nuclide calculation methods are included in the Supplemental Information.

The erosion rates have been recalculated to be internally consistent using the CRONUScalc program (Marrero et al., 2016a) and CRONUS-Earth production rates (Borchers et al., 2016; Marrero et al., 2016b; Phillips et al., 2016). We exclude ^{3}He measured in quartz because of known problems with ^{3}He retention in quartz (Bruno et al., 1997; Graf et al., 1991) and ^{21}Ne measured in pyroxenes because ^{21}Ne in pyroxene is not supported by the current version of CRONUScalc (Marrero et al., 2016a). The production rate used for ^{21}Ne in quartz is based on the ^{21}Ne/^{10}Be ratio presented in Balco and Shuster (2009). Fig. 3 shows a comparison between the recalculated and originally reported erosion rates for all nuclides. The apparent systematic differences primarily stem from changes in the common production rates used to calculate erosion rates, which manifests as a change in slope between a visual trend in the data and the dashed 1:1 line on the plot in Fig. 3 (Balco et al., 2008; Borchers et al., 2016; Heyman, 2014; Phillips et al., 2016).

In this study, results from different nuclides are compared, which may add uncertainty due to differences in both the production rates and half-life, the latter affecting the time periods over which erosion rates are applicable. We note that each nuclide will integrate erosion rates over different time periods, but suggest any temporal variations in erosion rates over the averaging timescale of the nuclides are likely to be small in the polar climate of Antarctica. The calculator, CRONUScalc, was originally calibrated across multiple nuclides (^{10}Be, ^{26}Al, ^{3}He, and ^{36}Cl) measured at a range of sites where at least two nuclides had been used, meaning that comparisons across nuclides should be reliable. ^{21}Ne, which was not included in the original CRONUScalc calibration, produces very similar rates compared to ^{10}Be, although sometimes these are slightly higher (Fig. 3). In studies where replicates were run for the same nuclide, the final recalculated erosion rates were averaged and those average values (with propagated uncertainties) were used in the final statistical analyses. Statistical analyses were performed using R (R Core Team, 2018).

Cosmogenic nuclide erosion rates are comparable across studies due to common collection criteria whereby ideal samples come from exposed, flat areas with no horizon obstructions and areas which have minimal chance of being covered by glacial drift in the past. The erosion rates from different studies on the same landform compare favourably (e.g. Fig. 4 showing Wright Valley and Mt. Fleming), indicating confidence in the reproducibility of these results. While the results of individual studies should be comparable to one another, preference of samples from stable, flat, topographic highs leads to the selection of preferentially more resistant parts of the landscape, meaning that these erosion rates are not directly comparable to, and are systematically lower than, those measured using other techniques or those collected at the basin scale (Bierman, 1994; Portenga and Bierman, 2011).

Limitations of this analysis stem from the availability of data, primarily the unequal number of data points in different geographic locations and the fact that few studies reported all the factors that may affect erosion rate (e.g. joint spacing or rock strength; Portenga and Bierman, 2011). Joint spacing is mainly relevant in temperate areas due to its potential to influence erosion through chemical dissolution and freeze-thaw processes. Secondly, these results have the potential to be geographically specific. For

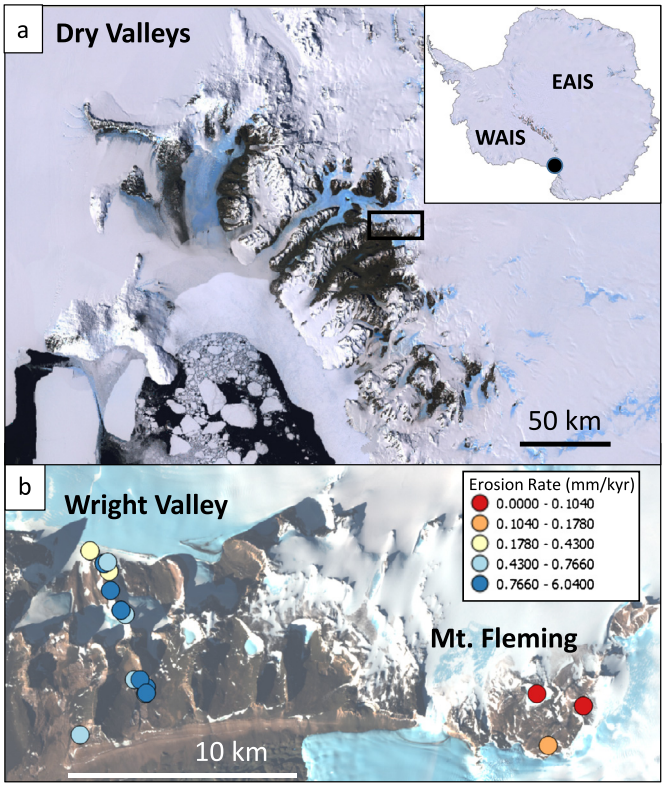

Fig. 4. Sample reproducibility comparison: location and results. (a) Location map showing the site in the Dry Valleys, East Antarctica (inset). (b) Erosion rates of two distinct groups of samples. The Wright Valley samples are from three studies: Balco et al. (2014), Nishiizumi et al. (1991), Middleton et al. (2012). The Mt. Fleming samples are from three studies: Schaefer et al. (1999), Summerfield et al. (1999), and Brook et al. (1995). (For interpretation of the colours in the figure(s), the reader is referred to the web version of this article.)

example, the Beacon Sandstone is likely to be over-represented compared to other sandstone formations due to its prevalence in the Dry Valleys, where many studies have been conducted. The potential effect is explored in the Supplemental Material, but none of the main conclusions of this paper are affected by the removal of any one study.

The potential effects of precipitation were not assessed in this study due to a lack of sufficiently accurate precipitation data. Precipitation values from accumulation models (effective resolution of ~100 km; Arthern et al., 2006) are not available with a resolution good enough to resolve differences between Dry Valleys locations at the coast and those 60 km inland at high elevation (which represent a range of precipitation values from 100+ mm/yr water equivalent down to <10 mm/yr (Summerfield et al., 1999)). Based on the aridity and low air temperatures of the study areas, we believe that precipitation (almost completely in solid form) is unlikely to have a significant effect on the erosion rates in this study, although this was not specifically tested. For example, almost all of the Dry Valleys samples in this compilation are located in Zone 3 of Marchant and Denton (1996), which suggests that liquid water is rare and that this area has remained a cold, desert environment for at least 10–15 Ma (Denton et al., 1993).

Although some lithologies are only represented by a small number of studies, sandstone, dolerite, and granite have large enough sample sizes to permit additional statistical evaluation within the populations. Granulite, quartzite, gneiss, and diorite are each only represented by a single study and are therefore not considered in detail.

Finally, not all studies reported lithology. Samples with unspecified lithology were compared to the ranges of erosion samples with reported lithologies; however, the unspecified samples do not appear to represent any distinct group that is different from those already represented in the compiled data set. The unspecified samples were therefore excluded from lithologic comparison but were included in other statistical analyses.

3. Carbonate erosion rate results & discussion

Individual erosion rate results for each sample are presented in Table 2, calculated using both the Lal (1991)/Stone (2000) scaling method (denoted ST) and the physics-based, nuclide-dependent scaling method from Lifton et al. (2014) (denoted LSDn). LSDn results are systematically 22–30% higher than those from ST scaling. All previous Antarctic erosion rate papers report results using Lal/Stone scaling, so we continue the analysis using only results calculated with that method for consistency. The statistical conclusions in this paper are based on relative differences between populations and do not change significantly with a different scaling model. In order to use these values to adjust exposure ages, the same scaling method should be used for both erosion rate and exposure calculations.

The minimum exposure erosion rate result from Mt. Fordell (0.23 ± 0.20 mm/ka) is almost identical to that of the infinite age scenario (0.27 ± 0.18 mm/ka) because the ^{36}Cl samples are essentially saturated after constant exposure for 1.4 Ma (Hein et al., 2016b). At Marble Dome, the minimum-exposure scenario results in ^{36}Cl samples that are saturated at zero erosion, meaning that zero erosion is the minimum boundary at this location. The average maximum erosion rate for Marble Dome is 0.20 ± 0.02 mm/ka. The erosion rates at the Mt. Fordell and Marble Dome sites are within uncertainty of each other, suggesting that the samples are likely saturated with respect to the erosion rate and that they provide a good estimate of the carbonate erosion rate in this region. Given the closeness to saturation, small changes in concentrations can result in significant changes in resulting erosion rates, as seen with the MH12-30 replicates. Combining the Mt. Fordell and Marble Dome samples yields minimum and maximum bounds of 0 mm/ka and 0.22 ± 0.02 mm/ka (ST scaling), and 0 mm/ka and 0.42 ± 0.02 mm/ka (LSDn scaling).

It is not possible to determine a well-defined exposure history for the other bedrock samples, so these are calculated for the infinite exposure assumption only in Table 2. The striated and polished bedrock samples collected at the ice margin yields an apparent, infinite-exposure erosion rate of ~100 mm/ka, with apparent erosion rates decreasing with increasing elevation (Fig. 5) until the limiting subaerial erosion rate is reached at high elevations. This trend reflects field evidence that apparent erosion rates close to the current ice elevation are higher due to increased erosion at the margin and/or repeated burial during glacial cycles, both of which would have a similar effect of lowering cosmogenic ^{36}Cl concentrations. This supports our approach of defining 'simple' exposure regions (Marble Dome and Mt. Fordell) based on ^{10}Be and ^{26}Al-dated erratics and relying only on ^{36}Cl erosion rate samples located in those regions to provide the best estimate of the carbonate erosion rate in the Marble Hills.

3.1. Carbonate erosion rate comparison

The limited number of previous ^{36}Cl carbonate bedrock studies report denudation rates at sites around the world ranging from 1–185 mm/ka (Evans, 2001; Fig. 1 references in Levenson et al., 2017). The large range of variability shown by these studies is attributed to climate trends in temperature and precipitation. Given the relative lack of liquid water in Antarctica, perhaps the most comparable sites to our results come from desert environments. For example, denudation rates from hyper-arid environments in

Table 2
Maximum erosion rates and uncertainties (mm/ka) for sites in the Marble Hills presented for two scaling schemes: Lal (1991)/Stone (2000) (ST) and the nuclide-dependent Lifton et al. (2014) (LSDn). Marble Dome and Mt. Fordell sites are presented for both infinite exposure and minimum exposure assumptions. Minimum exposure uses exposure ages from ^{10}Be and ^{26}Al (Marble Dome is 630 ka (LSDn)/660 ka (ST); Mt. Fordell is 1300 ka (LSDn)/1350 ka (ST)) in the calculation of the erosion rate for the ^{36}Cl samples. Uncertainties account for only the ^{36}Cl concentration, stable Cl concentration, and the production rate uncertainties, and full uncertainties, as detailed in Marrero et al. (2016b), are approximately 20–40% higher than those presented here (Supplementary Spreadsheet). The mean (replicates weighted at 0.5) and error of the mean is given for the Marble Dome site as well as all the simple exposure samples (Marble Dome and Mt. Fordell). MH12-30A and B are replicates processed with different ratios of carrier to sample.

	Elev above ice (m)	ST scaling		LSDn scaling	
		Inf. exposure	Known exposure	Inf. exposure	Known exposure
MH12-68	1005	0.27 ± 0.18	0.23 ± 0.20	0.48 ± 0.16	0.45 ± 0.16
MH12-30A	572	0.08 ± 0.19		0.27 ± 0.14	
MH12-30B	572	0.26 ± 0.18		0.45 ± 0.15	
MH12-31	572	0.23 ± 0.19		0.57 ± 0.17	
MH12-32	572	0.16 ± 0.22		0.38 ± 0.17	
MH12-C1-TO	584	0.25 ± 0.21		0.44 ± 0.18	
Marble Dome Mean		***0.20 ± 0.02***		***0.40 ± 0.02***	
Simple Exposure Mean		***0.22 ± 0.02***		***0.42 ± 0.02***	
MH14-13	534	0.50 ± 0.21		0.71 ± 0.18	
MH14-31	464	0.38 ± 0.20		0.57 ± 0.17	
MH12-75	400	0.59 ± 0.21		0.81 ± 0.18	
MH14-15	260	2.08 ± 0.37		2.43 ± 0.32	
MH14-38	151	8.4 ± 1.0		9.33 ± 0.88	
MH14-21	134	10.9 ± 1.3		12.1 ± 1.1	
MH14-37	43	99 ± 10		108.9 ± 9.1	

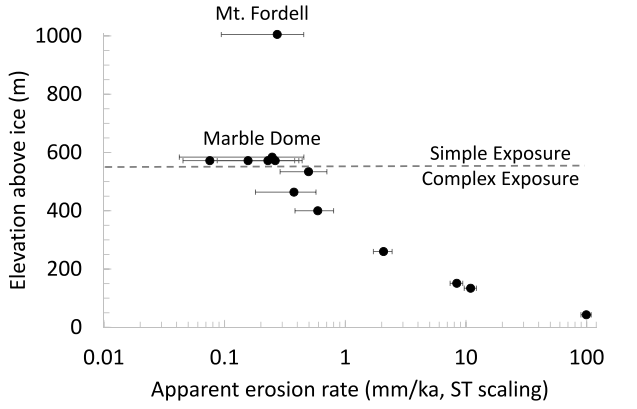

Fig. 5. Erosion rates for the Marble Hills carbonate bedrock samples derived from cosmogenic ^{36}Cl. Simple and complex exposure determined from ^{10}Be/^{26}Al erratic analyses in previous studies (Hein et al., 2016a, 2016b). All data taken from Table 2 and the Supplementary Spreadsheet.

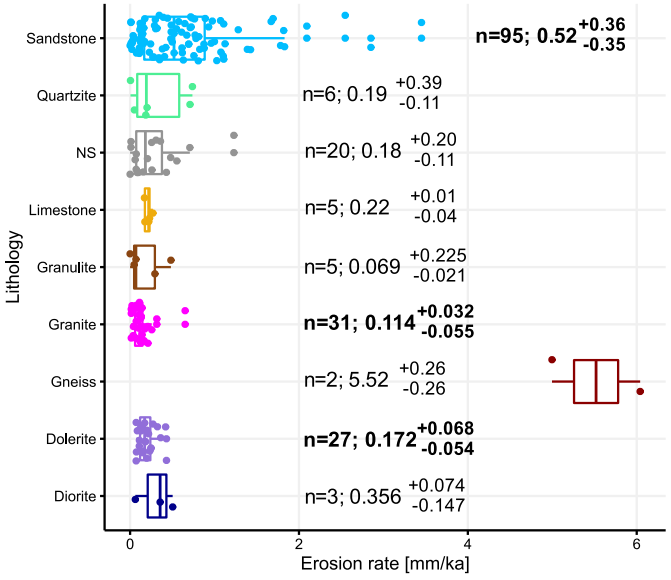

Fig. 6. Comparison of erosion rates by lithology. Number of samples for each category (n) has been listed along with the median, first quartile, and third quartiles (as shown in the box plot). Bold values indicate statistically significant sample populations. Mean and standard deviation provided in the Supplementary Spreadsheet.

Israel ranged from 1–3 mm/ka (Ryb et al., 2014) while reported denudation rates from arid Australia were 4.5 mm/ka (Stone et al., 1994). The erosion rates from Marble Hills are an order of magnitude lower than these values. While the difference between these rates may be minimal for some purposes, for a sample exposed for approximately 100 ka, the difference between an erosion rate of 0.2 mm/ka and erosion rates of 1 and 4 mm/ka can lead to a 6% and 68% change in calculated age, respectively. The new ^{36}Cl erosion rates reported in this study follow the global trend, where the erosion rates reported in Antarctica are among the lowest reported in the world for a given lithology (Portenga and Bierman, 2011).

4. Erosion rate compilation results and discussion

As expected, Antarctic erosion rates are low, with 87% of reported values lower than 1 mm/ka and 97% lower than 2 mm/ka. Because these values are maximum boundaries, true erosion rates may be even lower than those reported here. Beyond this, the statistical analysis of the data is used to investigate potential erosion rate differences due to lithology, boulder samples as opposed to bedrock, and sediment supply. Other parameters (elevation, temperature, latitude, publication year, coastal location, effect of removing individual studies) were investigated, but were not found to be significant (results and discussion in the Supplemental Information).

4.1. Lithology dependence

The compiled Antarctic erosion rates show a statistically significant dependence on lithology (Fig. 6). Sandstone shows the largest spread of erosion rates (0–3.5 mm/ka), while most other lithologies have tighter groupings within each lithology. The sandstone group (mean: 0.67 mm/ka) is distinguishable from all three other groups (Games-Howell, p-value = 0; Games-Howell does not re-

quire equal samples sizes or variances). Granite and dolerite populations have slightly different means (0.13 mm/ka and 0.19 mm/ka, respectively), but are not statistically distinguishable from one another (Games-Howell p-value of 0.16). The carbonate erosion rate is statistically distinguishable from the granite (Games-Howell, p-value $= 0.04$) and sandstone populations but not from dolerite. The mean carbonate erosion rate is slightly higher than that of granite or dolerite, but falls within the spread of the sandstone erosion rates.

The degree of cementation in individual samples could contribute to the large spread of sandstone erosion rates. Variable cementation in sandstone has been shown to result in a large range of abrasion rates in flume experiments (Attal and Lavé, 2009; Sklar and Dietrich, 2001). Ivy-Ochs et al. (1995) specifically note that they sampled 'silicified sandstone' from the Beacon Sandstone formation, while other authors listed the lithology from the same formation as simply 'sandstone'. This difference potentially indicates a range of cementation present in this lithology and may explain some of the variability in sandstone erosion rates. The three samples listed as 'silicified sandstone' yield results at the lower range of the sandstone values, but these are not separated out as a distinct lithology. Flume experiments of pebble abrasion also appear to be consistent with the results from this study: in the flume experiments, average limestone abrasion rates were slightly higher than average granite or volcanic abrasion rates and the limestone rates fell within the range of sandstone pebble abrasion rates, which had the largest range of abrasion rates in the study (Attal and Lavé, 2009). These results are also consistent with flume experiments of bedrock abrasion by sediment by Sklar and Dietrich (2001), and with Portenga and Bierman's (2011) compilation of worldwide ^{10}Be erosion rates, which showed higher global average erosion rates in outcrops made of sedimentary rocks, compared to igneous or metamorphic rocks.

The compiled cosmogenic nuclide data set can also be compared to two sets of Antarctic studies performed using microerosion meters (MEM) and mass loss calculations. MEM measurements over four years in the Larsemann and Vestfold Hills (Eastern Antarctica) revealed high erosion rates of 15 and 22 mm/ka (Spate et al., 1995). Lithologic differences were evident in samples exposed in the Allan Hills and the Dry Valleys, with a non-welded tuff eroding an order of magnitude faster than a dolerite sample (Malin, 1992). However, the five-year average erosion rates on the dolerite samples (3.3 mm/ka) are also significantly higher than those found using cosmogenic nuclides (0.20 mm/ka). The higher erosion rates recorded by the erosion meters could be due to the time scale of measurements, which may result in the erosion meter recording effects from individual large storms or other major events. Another possibility, particularly relevant in Antarctica, is that endolithic organisms or other processes may be acting over very long time scales to help create a resistant/armored surface or varnish that reduces erosion after an initial high-erosion period (de la Rosa et al., 2012). Finally, fundamental differences between the two techniques (e.g., sample selection/location) may lead to differences between the resulting rates. There are significant spatial differences in erosion rate in the Antarctic landscape (Matsuoka et al., 2006) and due to the choice of resistant outcrops for cosmogenic nuclide sampling, a comparatively lower erosion rate is expected for these surfaces when compared to other methods and/or erosion rates at the basin scale (e.g., Portenga and Bierman, 2011).

4.2. Boulder vs bedrock erosion rates

When subdivided by lithology, further examination into sample type indicates that there is a significant difference between bedrock and boulder samples, with boulder samples yielding systematically lower erosion rates (see Fig. 7 where the median of each population lies beyond the interquartile range of the other). For the purpose of this discussion, 'boulder' is considered to be any sample that was not attached to the bedrock. For sandstone, the median (0.12 mm/ka) and variance of boulder erosion rates lies within the lower range of the bedrock samples (below 1st quartile of 0.29 mm/ka). A similar difference is seen in dolerite boulder and bedrock populations, despite generally being an order of magnitude lower than the sandstone values. The difference in means is supported by statistically significant results ($p = 5.4 \times 10^{-11}$ for sandstone; $p = 0.0035$ for dolerite) from the Welch's two sample t-test, which accounts for differences in sample size. These differences are seen in the aggregated data, but can also be seen within individual studies, two of which are plotted individually in Fig. 7c (Margerison et al., 2005; Schaefer et al., 1999).

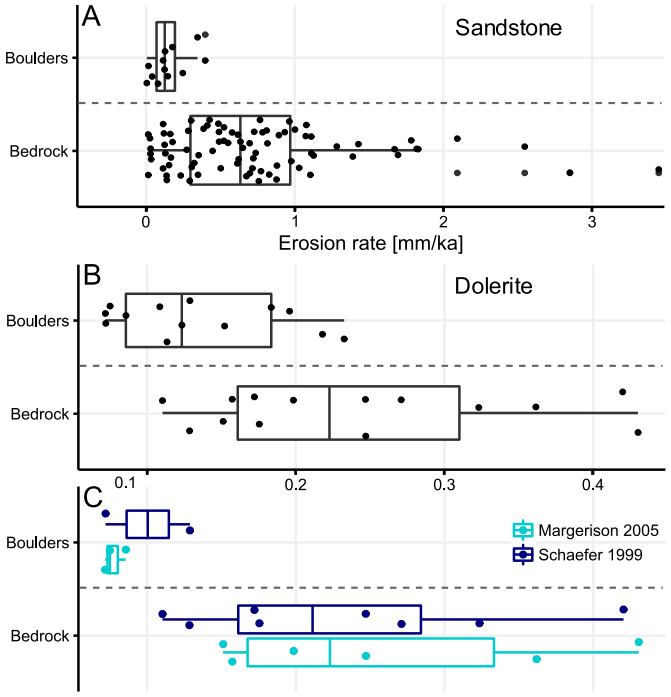

Fig. 7. Comparison between bedrock and boulders for two lithologies: sandstone (A) and dolerite (B). Boxplots show first quartile/median/third quartile. Note change of scale on x-axis between (A) and (B). (C) Two comparisons of boulder vs bedrock erosion rates in individual studies.

There are at least two plausible explanations for the generally higher values and larger spread for bedrock erosion rates as compared to those from boulders. First, repeated loading and unloading of rock due to glacial cycles may increase stress and create fractures in the rock, leading to increased erosion (Ziegler et al., 2013). In Antarctica, a preference for sampling small, glacially shaped boulders means that the samples have had weak areas eroded, leaving only the coherent (e.g. more resistant) boulder. In this scenario, bedrock would be less resistant to erosion than boulders. For similar reasons, bedrock surfaces are also more likely than boulders to retain the small amounts of liquid water that are present in the environment in the outcrop's more numerous joints and other discontinuities. This difference in moisture conditions was observed by Weed and Norton (1991), who differentiated between moisture regimes for Antarctic Beacon Supergroup sandstone bedrock and boulders, finding that increased water retention would lead to higher observed erosion rates in bedrock as compared to boulders.

A second potential explanation for the differences in bedrock/boulder erosion rates is ice coverage. If surfaces are covered by ice for extended periods of time (e.g. by cold-based (non-erosive) ice),

the maximum apparent erosion rate will increase due to shielding and lack of production during periods of burial, even though the subaerial erosion rate during exposure periods remains low. As a result, boulders may have significantly different exposure histories compared to bedrock, with boulders being more likely to have been eroded, transported, then exposed at the end of a glacial cycle. Bedrock on the other hand, may have survived several periods of glaciation, which could increase the variability in apparent cosmogenic nuclide erosion rates. We consider it likely that both physical processes and glacial history effects combine to yield the consistently lower erosion rates observed in boulders when compared to those from bedrock samples.

4.3. Erosion processes in Antarctica

Erosion rates from the Dry Valleys are generally higher than those from other locations on the continent, particularly for sandstone (Fig. 8). A similar trend is seen for dolerite, although it is less significant due to the smaller initial spread in erosion rates and smaller sample size. The Dry Valleys region is a unique site in Antarctica, where there is an abundant ice-free sediment supply. Erosion through wind-driven abrasion with sediment particles could therefore explain the higher erosion rates in the Dry Valleys compared to other areas in Antarctica, which are primarily abraded by ice crystals (rather than sediment). Plentiful ventifacts in and around the Dry Valleys (Marchant and Denton, 1996) suggest long-term erosion by wind-driven particles, whilst modern observations of 'wind-blown sand' (Marchant and Head, 2007) in the region point to the importance of sediment supply. Observations of identical rock samples placed in different Antarctic locations support this hypothesis (Malin, 1988, 1992). Samples placed in areas where loose and mobile sediment was available on neighbouring hillsides (as in the Dry Valleys) were abraded at higher rates than samples placed on a blue ice area in the Allan Hills, where it was suspected that only ice crystals were available to abrade the surface samples.

Our data suggest that granular or mineral-scale processes are dominant for these sample types based on the similarity between erosion rates of limestone, granite, and dolerite populations. Erosion processes likely include mechanical processes such as abrasion and granular disintegration (Stone et al., 1994). The effect of larger-scale freeze-thaw for this type of landform in Antarctica is small compared to alpine locations, based on the very low and consistent erosion rates. Freeze-thaw operates on the scale of natural joint spacing in the rock, which typically results in large erosion rate variability. Indeed, if a large piece of rock was recently removed due to freeze-thaw or other similar process (e.g. thermal shock), a significantly higher erosion rate should be recorded in at least some samples due to the lowered nuclide concentration. This seems unlikely, especially for granite and dolerite lithologies, which show tight groupings of erosion rates.

5. Global comparisons

On a global scale, only cosmogenic nuclide-derived erosion rates from the driest part of the Atacama Desert (0.2–0.4 mm/ka; Placzek et al., 2010) and South Africa (1–6 mm/ka, depending on lithology and climate; Fleming et al., 1999; Kounov et al., 2007) have yielded results similar to the extremely low rates in Antarctica. The similarly low rates across lithologies in arid environments support our interpretation that weathering in these environments is almost exclusively by mechanical processes, even for carbonates.

Results from this study are compared to trends found during the compilation of global ^{10}Be erosion rate data by Portenga and Bierman (2011), who analysed bedrock outcrop data from a variety of regions across the world (although the proportion of polar data in the study was small, at just 7%). Over global data sets,

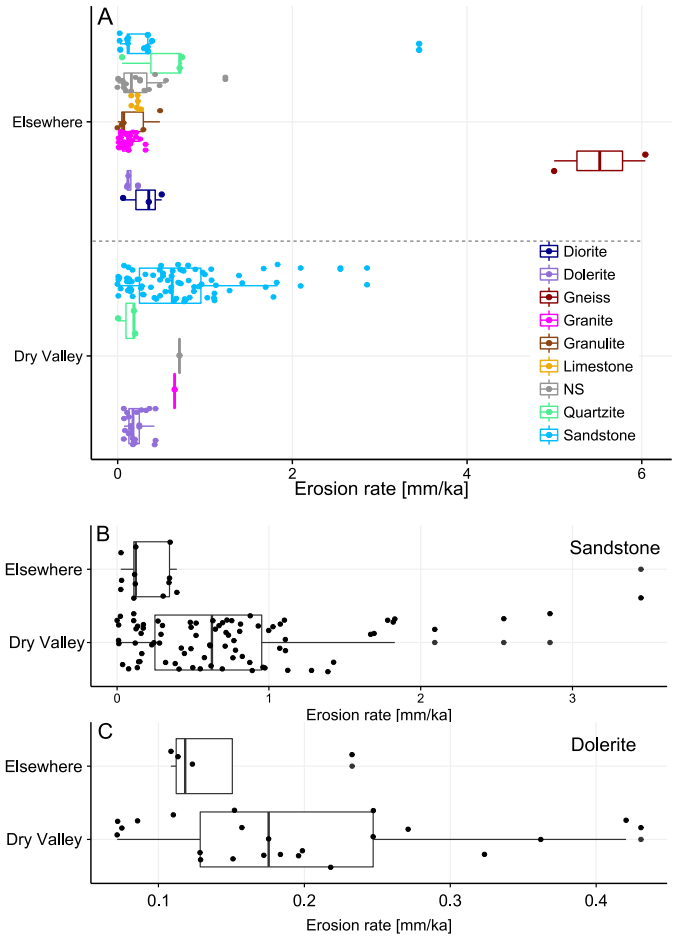

Fig. 8. Erosion rates by location, comparing samples from the Dry Valleys and elsewhere on the continent. All samples are shown in panel (a), with individual rock types shown in panels (b) sandstone and (c) dolerite.

outcrop erosion rates differed by climate and rock type (i.e. sedimentary, igneous, metamorphic), with rates also weakly correlated with relief and annual precipitation. Polar outcrops were the slowest eroding and (when combined with arid and cold outcrops) only a few weakly correlated parameters showed any influence on erosion rate in these regions. These included elevation, mean annual precipitation, and latitude. In addition to these variables (excluding precipitation), we also tested the influence of other potentially relevant variables – including distance to the coast, (potentially a proxy for change in precipitation, wind speed, or temperature as is seen in other climate regimes), and publication year (potentially reflecting technical advancements that produced a systematic change in reported erosion rates). However, we found no consistent trends in erosion rate with respect to elevation (Fig. S15), publication year (Fig. S16), coastal location (Fig. S17), temperature (Fig. S21), or latitude (Fig. S22).

6. Conclusion

The new ^{36}Cl carbonate bedrock erosion rate determined from Marble Hills, of 0.22 $\pm$ 0.02 mm/ka (infinite exposure, maximum limit, ST scaling), is lower than previous cosmogenic nuclide-derived carbonate erosion rates determined in desert environments elsewhere in the world. Our carbonate erosion rate is placed in context through a compilation and reanalysis of 28 Antarctic studies that produced cosmogenic nuclide-derived erosion rates from other nuclides. The mean and spread of erosion rates from

other lithologies (limited to those with a statistically significant number of measurements) are also provided, with means and 1st/3rd quartiles of 0.11 +0.03/−0.06 mm/ka for granite, 0.17 +0.07/−0.05 mm/ka for dolerite, and 0.52 +0.36/−0.35 mm/ka for sandstone. Our new carbonate value is similar to the range of erosion rates from these other lithologies, which suggests that the inefficiency of chemical weathering in cold, dry environments can help to explain consistently low erosion rates across lithologies in Antarctica.

Based on analysis of the erosion rate compilation, this study finds that rock type (to some degree) and sample type (boulder vs bedrock) control reported cosmogenic nuclide-derived erosion rates in Antarctica. This finding helps to explain erosion rate variability in outcrops across the continent. Our results also suggest that sediment availability can influence erosion rates through wind-driven abrasion.

Author contributions

SMM, ASH, DES, JW, KW, SD all participated in field work and collection of samples. MN and SMM performed statistical analyses. SMM physically prepared and chemically processed samples and RS performed the AMS analyses of the samples. All authors assisted SMM on the manuscript and have approved the final version of this manuscript.

Acknowledgements

The research was supported by the UK Natural Environment Research Council: Grant numbers NE/1025840/1, NE/1034194/1 and NE/G013071/1. Thanks to K. Hippe for a useful review. We thank the British Antarctic Survey for logistical and field support. Thanks to F. Christie for help with figures and A. Rodés and A. Van der Geest for technical discussions. Funding sources were not involved with any decisions about this project after the funding was initially approved.

Appendix A. Supplementary material

Supplementary material related to this article can be found online at https://doi.org/10.1016/j.epsl.2018.08.018.

References

Ackert Jr., R.P., 1999. Measurements of past ice sheet elevations in interior West Antarctica. Science 286 (5438), 276–280.

Ackert, R.P., Kurz, M.D., 2004. Age and uplift rates of Sirius Group sediments in the Dominion Range, Antarctica, from surface exposure dating and geomorphology. Glob. Planet. Change 42 (1–4), 207–225.

Altmaier, M., Herpers, U., Delisle, G., Merchel, S., Ott, U., 2010. Glaciation history of Queen Maud Land (Antarctica) reconstructed from in-situ produced cosmogenic ^{10}Be, ^{26}Al and ^{21}Ne. Polar Sci. 4 (1), 42–61.

Arthern, R.J., Winebrenner, D.P., Vaughan, D.G., 2006. Antarctic snow accumulation mapped using polarization of 4.3-cm wavelength microwave emission. J. Geophys. Res. 111 (D6).

Attal, M., Lavé, J., 2009. Pebble abrasion during fluvial transport: experimental results and implications for the evolution of the sediment load along rivers. J. Geophys. Res. 114 (F4).

Balco, G., Shuster, D.L., 2009. Production rate of cosmogenic ^{21}Ne in quartz estimated from ^{10}Be, ^{26}Al, and ^{21}Ne concentrations in slowly eroding Antarctic bedrock surfaces. Earth Planet. Sci. Lett. 281 (1–2), 48–58.

Balco, G., Stone, J.O., Lifton, N.A., Dunai, T.J., 2008. A complete and easily accessible means of calculating surface exposure ages or erosion rates from ^{10}Be and ^{26}Al measurements. Quat. Geochronol. 3 (3), 174–195.

Balco, G., Stone, J.O.H., Sliwinski, M.G., Todd, C., 2014. Features of the glacial history of the Transantarctic Mountains inferred from cosmogenic ^{26}Al, ^{10}Be and ^{21}Ne concentrations in bedrock surfaces. Antarct. Sci. 26 (06), 708–723.

Bentley, M.J., Fogwill, C.J., Le Brocq, A.M., Hubbard, A.L., Sugden, D.E., Dunai, T.J., Freeman, S.P.H.T., 2010. Deglacial history of the West Antarctic Ice Sheet in the Weddell Sea embayment: constraints on past ice volume change. Geology 38 (5), 411–414.

Bierman, P.R., 1994. Using in situ produced cosmogenic isotopes to estimate rates of landscape evolution: a review from the geomorphic perspective. J. Geophys. Res. 99 (B7), 13885.

Bierman, P.R., Caffee, M., 2002. Cosmogenic exposure and erosion history of Australian bedrock landforms. GSA Bull. 114 (7), 787–803. https://doi.org/10.1130/0016-7606(2002)114<0787:CEAEHO>2.0.CO;2.

Bierman, P.R., Steig, E.J., 1996. Estimating rates of denudation using cosmogenic isotope abundances in sediment. Earth Surf. Process. Landf. 21, 125–139.

Borchers, B., Marrero, S., Balco, G., Caffee, M., Goehring, B.M., Gosse, J., Lifton, N., Nishiizumi, K., Phillips, F.M., Schaefer, J., Stone, J.O., 2016. Geological calibration of spallation production rates in the CRONUS-Earth project. Quat. Geochronol. 31, 188–198.

Bookhagen, B., Strecker, M.R., 2012. Spatiotemporal trends in erosion rates across a pronounced rainfall gradient: examples from the southern Central Andes. Earth Planet. Sci. Lett. 327–328, 97–110.

Bromley, G.R.M., Hall, B.L., Stone, J.O., Conway, H., Todd, C.E., 2010. Late Cenozoic deposits at Reedy Glacier, Transantarctic Mountains: implications for former thickness of the West Antarctic Ice Sheet. Quat. Sci. Rev. 29 (3–4), 384–398.

Brook, E.J., Brown, E.T., Kurz, M.D., Ackert, R.P., Raisbeck, G.M., Yiou, F., 1995. Constraints on age, erosion, and uplift of Neogene glacial deposits in the Transantarctic Mountains determined from in situ cosmogenic ^{10}Be and ^{26}Al. Geology 23 (12), 1063.

Brown, E.T., Edmond, J.M., Raisbeck, G.M., Yiou, F., Kurz, M.D., Brook, E.J., 1991. Examination of surface exposure ages of Antarctic moraines using in situ produced ^{10}Be and ^{26}Al. Geochim. Cosmochim. Acta 55, 2269–2283.

Bruno, L.A., Baur, H., Graf, T., Schluchter, C., Signer, P., Wieler, R., 1997. Dating of Sirius Group tillites in the Antarctic Dry Valleys with cosmogenic ^{3}He and ^{21}Ne. Earth Planet. Sci. Lett. 147, 37–54.

de la Rosa, J.P.M., Warke, P.A., Smith, B.J., 2012. Lichen-induced biomodification of calcareous surfaces: bioprotection versus biodeterioration. Prog. Phys. Geogr. 37 (3), 325–351.

Denton, G.H., Sugden, D.E., Marchant, D.R., Hall, B.L., Wilch, T.I., 1993. East Antarctic Ice Sheet sensitivity to Pliocene climatic change from a Dry Valleys perspective. Geogr. Ann. 75 (4), 155–204.

Di Nicola, L., Baroni, C., Strasky, S., Salvatore, M.C., Schlüchter, C., Akçar, N., Kubik, P.W., Wieler, R., 2012. Multiple cosmogenic nuclides document the stability of the East Antarctic Ice Sheet in northern Victoria Land since the Late Miocene (5–7 Ma). Quat. Sci. Rev. 57, 85–94.

Evans, J.M., 2001. Calibration of the Production Rates of Cosmogenic ^{36}Cl from Potassium. Doctorate of Philosophy. The Australian National University, 142 p.

Fink, D., McKelvey, B., Hambrey, M., Fabel, D., Brown, R., 2006. Pleistocene deglaciation chronology of the Amery Oasis and Radok Lake, northern Prince Charles Mountains, Antarctica. Earth Planet. Sci. Lett. 243 (1–2), 229–243.

Fleming, A., Summerfield, M.A., Stone, J.O., Fifield, L.K., Cresswell, R.G., 1999. Denudation rates for the southern Drakensberg escarpment, SE Africa, derived from in-situ-produced cosmogenic ^{36}Cl: initial results. J. Geol. Soc. Lond. 156, 209–212.

Fogwill, C.J., Bentley, M.J., Sugden, D.E., Kerr, A.R., Kubik, P.W., 2004. Cosmogenic nuclides ^{10}Be and ^{26}Al imply limited Antarctic Ice Sheet thickening and low erosion in the Shackleton Range for >1 m.y. Geology 32 (3), 265.

Graf, T., Kohl, C.P., Marti, K., Nishiizumi, K., 1991. Cosmic-ray produced neon in Antarctic rocks. Geophys. Res. Lett. 18 (2), 203–206.

Granger, D.E., Kirchner, J.W., Finkel, R., 1996. Spatially averaged long-term erosion rates measured from in situ-produced cosmogenic nuclides in alluvial sediment. J. Geol. 104, 249–257.

Harel, M.A., Mudd, S.M., Attal, M., 2016. Global analysis of the stream power law parameters based on worldwide ^{10}Be denudation rates. Geomorphology 268, 184–196.

Heimsath, A.M., Dietrich, W.E., Nishiizumi, K., Finkel, R.C., 1999. Cosmogenic nuclides, topography, and the spatial variation of soil depth. Geomorphology 27 (1–2), 151–172. https://doi.org/10.1016/S0169-555X(98)00095-6.

Hein, A.S., Marrero, S.M., Woodward, J., Dunning, S.A., Winter, K., Westoby, M.J., Freeman, S.P.H.T., Shanks, R.P., Sugden, D.E., 2016a. Mid-Holocene pulse of thinning in the Weddell Sea sector of the West Antarctic Ice Sheet. Nat. Commun. 7, 12511.

Hein, A.S., Woodward, J., Marrero, S.M., Dunning, S.A., Steig, E.J., Freeman, S.P., Stuart, F.M., Winter, K., Westoby, M.J., Sugden, D.E., 2016b. Evidence for the stability of the West Antarctic Ice Sheet divide for 1.4 million years. Nat. Commun. 7, 10325.

Hewawasam, T., von Blanckenburg, F., Schaller, M., Kubik, P., 2003. Increase of human over natural erosion rates in tropical highlands constrained by cosmogenic nuclides. Geology 31 (7), 597–600.

Heyman, J., 2014. Paleoglaciation of the Tibetan Plateau and surrounding mountains based on exposure ages and ELA depression estimates. Quat. Sci. Rev. 91, 30–41.

Hodgson, D.A., Bentley, M.J., Schnabel, C., Cziferszky, A., Fretwell, P., Convey, P., Xu, S., 2012. Glacial geomorphology and cosmogenic ^{10}Be and ^{26}Al exposure ages in the northern Dufek Massif, Weddell Sea embayment, Antarctica. Antarct. Sci. 24 (04), 377–394.

Huang, F., Li, G., Liu, X., Kong, P., Ju, Y., Fink, D., Fang, A., Yu, L., 2010. Minimum bedrock exposure ages and their implications: Larsemann Hills and Neighboring Bolingen Islands, East Antarctica. Acta Geol. Sin. 84 (3), 543–548.

Ivy-Ochs, S., Schluchter, C., Kubik, P.W., Dittrich-Hannen, B., Beer, J., 1995. Minimum ^{10}Be exposure ages of early Pliocene for the Table Mountain plateau and the Sirius Group at Mount Fleming, Dry Valleys, Antarctica. Geology 23 (11), 1007–1010.

Kiernan, K., Gore, D.B., Fink, D., White, D.A., McConnell, A., Sigurdsson, I.A., 2009. Deglaciation and weathering of Larsemann Hills, East Antarctica. Antarct. Sci. 21 (04), 373.

Kounov, A., Niedermann, S., de Wit, M.J., Viola, G., Andreoli, M., Erzinger, J., 2007. Present denudation rates at selected sections of the South African escarpment and the elevated continental interior based on cosmogenic ^{3}He and ^{21}Ne. S. Afr. J. Geol. 110 (2–3), 235–248.

Lal, D., 1991. Cosmic ray labeling of erosion surfaces: in situ nuclide production rates and erosion models. Earth Planet. Sci. Lett. 104, 424–439.

Levenson, Y., Ryb, U., Emmanuel, S., 2017. Comparison of field and laboratory weathering rates in carbonate rocks from an Eastern Mediterranean drainage basin. Earth Planet. Sci. Lett. 465, 176–183.

Lifton, N., Sato, T., Dunai, T.J., 2014. Scaling in situ cosmogenic nuclide production rates using analytical approximations to atmospheric cosmic-ray fluxes. Earth Planet. Sci. Lett. 386, 149–160.

Lilly, K., Fink, D., Fabel, D., Lambeck, K., 2010. Pleistocene dynamics of the interior East Antarctic ice sheet. Geology 38 (8), 703–706.

Malin, M.C., 1988. Abrasion in ice-free areas of southern Victoria Land, Antarctica. Antarct. J., 38.

Malin, M.C., 1992. Short-term variations in the rate of Eolian processes, southern Victoria Land, Antarctica. Antarct. J. U.S. 26 (5), 27–29.

Marchant, D.R., Denton, G.H., 1996. Miocene and Pliocene paleoclimate of the Dry Valleys region, Southern Victoria land: a geomorphological approach. Mar. Micropaleontol. 27, 253–271.

Marchant, D.R., Head, J.W., 2007. Antarctic dry valleys: microclimate zonation, variable geomorphic processes, and implications for assessing climate change on Mars. Icarus 192 (1), 187–222.

Margerison, H.R., Phillips, W.M., Stuart, F.M., Sugden, D.E., 2005. Cosmogenic ^{3}He concentrations in ancient flood deposits from the Coombs Hills, northern Dry Valleys, East Antarctica: interpreting exposure ages and erosion rates. Earth Planet. Sci. Lett. 230 (1–2), 163–175.

Marrero, S., Phillips, F., Borchers, B., Lifton, N., Aumer, R., Balco, G., 2016a. Cosmogenic nuclide systematics and the CRONUScalc program. Quat. Geochronol. 31, 160–187.

Marrero, S., Phillips, F., Caffee, M., Gosse, J., 2016b. CRONUS-Earth cosmogenic ^{36}Cl calibration. Quat. Geochronol. 31, 199–219.

Matsuoka, N., Thomachot, C.E., Oguchi, C.T., Hatta, T., Abe, M., Matsuzaki, H., 2006. Quaternary bedrock erosion and landscape evolution in the Sør Rondane Mountains, East Antarctica: reevaluating rates and processes. Geomorphology 81 (3–4), 408–420.

Middleton, J.L., Ackert, R.P., Mukhopadhyay, S., 2012. Pothole and channel system formation in the McMurdo Dry Valleys of Antarctica: new insights from cosmogenic nuclides. Earth Planet. Sci. Lett. 355–356, 341–350.

Molnar, P., England, P., 1990. Late Cenozoic uplift of mountain ranges and global climate change: chicken or egg? Nature 346 (6279), 29–34.

Mukhopadhyay, S., Ackert, R.P., Pope, A.E., Pollard, D., DeConto, R.M., 2012. Miocene to recent ice elevation variations from the interior of the West Antarctic ice sheet: constraints from geologic observations, cosmogenic nuclides and ice sheet modeling. Earth Planet. Sci. Lett. 337–338, 243–251.

Niedermann, S., 2002. Cosmic-ray-produced noble gases in terrestrial rocks: dating tools for surface processes. Rev. Mineral. Geochem. 47, 731–784.

Nishiizumi, K., Kohl, C.P., Arnold, J.R., Klein, J., Fink, D., Middleton, J.L., 1991. Cosmic ray produced ^{10}Be and ^{26}Al in Antarctic rocks: exposure and erosion history. Earth Planet. Sci. Lett. 104, 440–454.

Oberholzer, P., Baroni, C., Salvatore, M.C., Baur, H., Wieler, R., 2008. Dating late Cenozoic erosional surfaces in Victoria Land, Antarctica, with cosmogenic neon in pyroxenes. Antarct. Sci. 20 (01), 89–98.

Oberholzer, P., Baroni, C., Schaefer, J.M., Orombelli, G., Ochs, S.I., Kubik, P.W., Baur, H., Wieler, R., 2003. Limited Pliocene/Pleistocene glaciation in Deep Freeze Range, northern Victoria Land, Antarctica, derived from in situ cosmogenic nuclides. Antarct. Sci. 15 (4), 493–502.

Peizhen, Z., Molnar, P., Downs, W.R., 2001. Increased sedimentation rates and grain sizes 2–4 Myr ago due to the influence of climate change on erosion rates. Nature 410, 891–897.

Phillips, F.M., Argento, D.C., Balco, G., Caffee, M.W., Clem, J., Dunai, T., Finkel, R., Goehring, B., Gosse, J.C., Hudson, A., Jull, T.A., Kelly, M., Kurz, M., Lal, D., Lifton, N., Marrero, S.M., Nishiizumi, K., Reedy, R., Schaefer, J., Stone, J.O., Swanson, T., Zreda, M.G., 2016. The CRONUS-Earth project: a synthesis. Quat. Geochronol. 31, 119–154.

Placzek, C.J., Matmon, A., Granger, D.E., Quade, J., Niedermann, S., 2010. Evidence for active landscape evolution in the hyperarid Atacama from multiple terrestrial cosmogenic nuclides. Earth Planet. Sci. Lett. 295 (1–2), 12–20.

Portenga, E.W., Bierman, P.R., 2011. Understanding Earth's eroding surface with ^{10}Be. GSA Today 21 (8), 4–10.

R Core Team, 2018. R: A Language and Environment for Statistical Computing. R Foundation for Statistical Computing, Vienna, Austria. https://www.R-project.org/.

Ryb, U., Matmon, A., Erel, Y., Haviv, I., Benedetti, L., Hidy, A.J., 2014. Styles and rates of long-term denudation in carbonate terrains under a Mediterranean to hyperarid climatic gradient. Earth Planet. Sci. Lett. 406, 142–152.

Schaefer, J.M., Ivy-Ochs, S., Wieler, R., Leya, I., Baur, H., Denton, G.H., Schluchter, C., 1999. Cosmogenic noble gas studies in the oldest landscape on earth: surface exposure ages of the Dry Valleys, Antarctica. Earth Planet. Sci. Lett. 167, 215–226.

Sklar, L.S., Dietrich, W.E., 2001. Sediment and rock strength controls on river incision into bedrock. Geology 29 (12), 1087–1090.

Spate, A.P., Burgess, J.S., Shevlin, J., 1995. Rates of rock surface lowering, Princess Elizabeth Land, Eastern Antarctica. Earth Surf. Process. Landf. 20, 567–573.

Staiger, J.W., Marchant, D.R., Schaefer, J.M., Oberholzer, P., Johnson, J.V., Lewis, A.R., Swanger, K.M., 2006. Plio-Pleistocene history of Ferrar Glacier, Antarctica: implications for climate and ice sheet stability. Earth Planet. Sci. Lett. 243 (3–4), 489–503.

Stephenson, W.J., Finlayson, B.L., 2009. Measuring erosion with the micro-erosion meter—contributions to understanding landform evolution. Earth-Sci. Rev. 95 (1–2), 53–62.

Stone, J., 2000. Air pressure and cosmogenic isotope production. J. Geophys. Res. 105 (B10), 23753–23760.

Stone, J.O., Allan, G.L., Fifield, L.K., Evans, J.M., Chivas, A.R., 1994. Limestone erosion measurements with cosmogenic chlorine-36 in calcite – preliminary results from Australia. Nucl. Instrum. Methods Phys. Res., Sect. B, Beam Interact. Mater. Atoms 92, 311–316.

Sugden, D.E., Hein, A.S., Woodward, J., Marrero, S.M., Rodés, Á., Dunning, S.A., Stuart, F.M., Freeman, S.P.H.T., Winter, K., Westoby, M.J., 2017. The million-year evolution of the glacial trimline in the southernmost Ellsworth Mountains, Antarctica. Earth Planet. Sci. Lett. 469, 42–52.

Summerfield, M.A., Sugden, D.E., Denton, G.H., Marchant, D.R., Cockburn, H.A.P., Stuart, F.M., 1999. Cosmogenic isotope data support previous evidence of extremely low rates of denudation in the Dry Valleys region, southern Victoria Land, Antarctica. Geol. Soc. (Lond.) Spec. Publ. 162 (1), 255–267.

Swanger, K.M., Marchant, D.R., Schaefer, J.M., Winckler, G., Head, J.W., 2011. Elevated East Antarctic outlet glaciers during warmer-than-present climates in southern Victoria Land. Glob. Planet. Change 79 (1–2), 61–72.

Tomkin, J.H., Brandon, M.T., Pazzaglia, F.J., Barbour, J.R., Willett, S.D., 2003. Quantitative testing of bedrock incision models for the Clearwater River, NW Washington State. J. Geophys. Res., Solid Earth 108 (B6).

van der Beek, P., Bishop, P., 2003. Cenozoic river profile development in the Upper Lachlan catchment (SE Australia) as a test of quantitative fluvial incision models. J. Geophys. Res., Solid Earth 108 (B6).

Weed, R., Norton, S.A., 1991. Siliceous crusts, quartz rinds and biotic weathering of sandstones in the cold desert of Antarctica. In: Berthelin, J. (Ed.), Diversity of Environmental Biogeochemistry. Elsevier, Amsterdam, Netherlands, pp. 327–339.

Weyant, W.S., 1966. The Antarctic Climate, Antarctic Soils and Soil Forming Processes. American Geophysical Union, pp. 47–59.

White, D.A., Bennike, O., Berg, S., Harley, S.L., Fink, D., Kiernan, K., McConnell, A., Wagner, B., 2009. Geomorphology and glacial history of Rauer Group, East Antarctica. Quat. Res. 72 (1), 80–90.

Ziegler, M., Loew, S., Moore, J.R., 2013. Distribution and inferred age of exfoliation joints in the Aar Granite of the central Swiss Alps and relationship to Quaternary landscape evolution. Geomorphology 201, 344–362.